Metal Nanoparticle Loaded Magnetic-Chitosan Microsphere: Water Dispersible and Easily Separable Hybrid Metal Nano-Biomaterial for Catalytic Applications

Thanusu Parandhaman,[a,c] Nagaraju Pentela,[b,c] Baskaran Ramalingam,[a] Debasis Samanta,[b,c] and Sujoy K. Das*,[a,c]

[a]Biological Materials Laboratory, [b]Polymer Science Division, Council of Scientific and Industrial Research (CSIR)-Central Leather Research Institute (CLRI), Chennai- 600020, India, [c]Academic of Scientific and Innovative Research (AcSIR), New Delhi-110001, India.

Biosynthesis of Magnetic Nanoparticle. The biogenic synthesis of magnetic nanoparticle was carried out following incubation of magnetite precursor, akaganeite (–FeOOH) with *S. algae* under anaerobic condition at 33 °C for 3 days. The magnetite precursor, akaganeite was initially prepared by neutralizing $FeCl_3.6H_2O$ (2 M) solution with NaOH (10 M) solution to make the pH 7.0 and stirred at 30 °C for overnight. The suspension was transferred in serum bottle and diluted in HEPES buffer (50 mM, pH 7.5) to make the final concentration of Fe(III) oxyhydroxide to 0.4 M followed by addition of 10 mM lactate as the electron donor. The *S. algae* cells were then added into serum bottle containing Fe(III) oxyhydroxide and lactate. The serum bottle was sealed tightly and purged with N_2 (100%) gas to maintain the anaerobic condition. The reaction mixture was then incubated at 33 °C for 3 days in dark condition. Following incubation the colour of the solution changed to black from initial brown and attracted by the external magnet.

Results

The decoration of Au and PdNPs on the surface of Fe_3O_4@Ch and subsequent formation of Fe_3O_4@Ch-AuNPs and Fe_3O_4@Ch-PdNPs was carried out through microwave assisted reduction of surface bound metal ions. In the process the dissolved oxygen reacted with hydroxyl group of Fe_3O_4@Ch and generate superoxide anions, which induced reduction of metal ions into metal nanoparticle (Au and PdNPs) possibly through the following steps:

*Address for communication: Dr. Sujoy K. Das, Email: sujoy@clri.res.in; sujoydasiacs@gmail.com. Tel: +914424437133. Fax: +914424910846.

$MY \longrightarrow M^+ + Y^-$

$M^+ + {}^-Fe_3O_4@Ch \longrightarrow M^+\text{-}Fe_3O_4@Ch$

$Fe_3O_4@Ch_{red} + O_2 \xrightarrow{\text{irradiation}} Fe_3O_4@Ch_{ox} + O_2^{\cdot -}$

$O_2^{\cdot -} + M^+\text{-}\ Fe_3O_4@Ch \xrightarrow{\text{reduction}} Fe_3O_4@Ch\text{-MNPs: M= Au or Pd}$

Scherrer equation

$$D_p = \frac{K\,\lambda}{\beta_{1/2}\cos\theta}$$

Where

D_p = Average crystallite size in Å, K = Shape factor, β = Full width at half maximum (FWHM) of the observed peak in radians, θ = Bragg diffraction angle in degrees, and λ = X-ray wavelength in Å

Before calcination:

$$D_p = \frac{0.94 * 1.54}{(0.34 * \frac{\pi}{180}) * \cos 17.7°} = 256.0\ \text{Å} = 25.6\ \text{nm}$$

After calcination:

$$D_p = \frac{0.94 * 1.54}{(0.30 * \frac{\pi}{180}) * \cos 17.75°} = 290.2\ \text{Å} = 29.0\ \text{nm}$$

The calcination process slightly increased the size of the magnetite nanoparticle from 25.6 nm to 29 nm. Moreover, the results showed that crystallite size determined from Scherrer equation was considerable same with the particle size measured from FESEM analysis.

XPS analysis

The analysis of core-level spectra of C 1s, N 1s and O 1s depicted protein signature associated with Fe_3O_4 nanoparticles. The C 1s spectrum (**Figure S1A**) showed binding energies at 284.2, 286.1, and 287.9 eV. The peak at 284.2 eV was attributed to C–C and C–H, whereas carbon bounded to nitrogen (C–N) and hydroxyl groups (C–OH) were located at 286.1 eV. The carboxylate (–C(=O)–OH) and amide carbon (N–C=O) groups were located at 287.9 eV. **Figure S1B** showed N1s core levels peaks with three chemically distinct species at 398.8, 400.4 and 401.8 eV. These correspond to amine (-NH-), imine (-C=N-) and protonated amine functional groups respectively, associated with Fe_3O_4 nanoparticle surface. Two distinct peaks at 532.2 and 533.8 eV in the O 1s spectrum (**Figure S1C**) represented the incorporation of C=O and C–OH components of protein moiety, respectively.

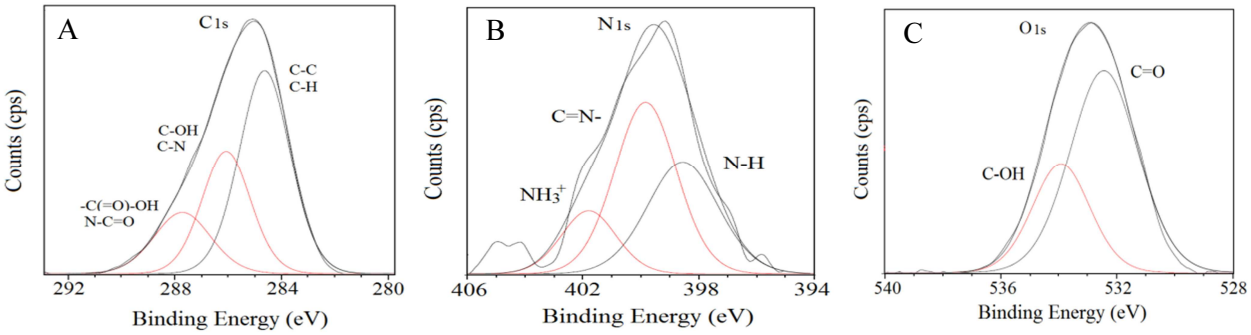

Figure S1: Core level XPS spectra of C 1s (A), N 1s (B) and O 1s (C) of the biosyntheized Fe_3O_4 nanoparticles.

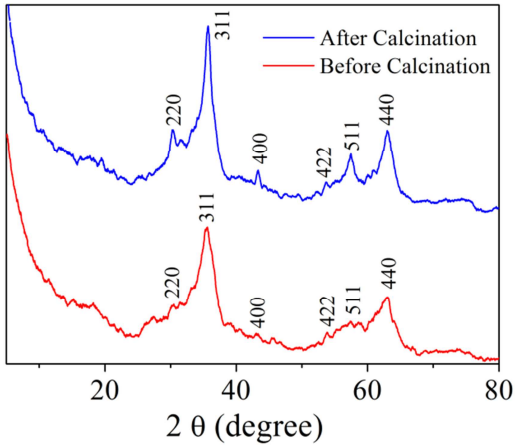

Figure S2: XRD of biosynthesized magnetic nanoparticles before and after calcination.

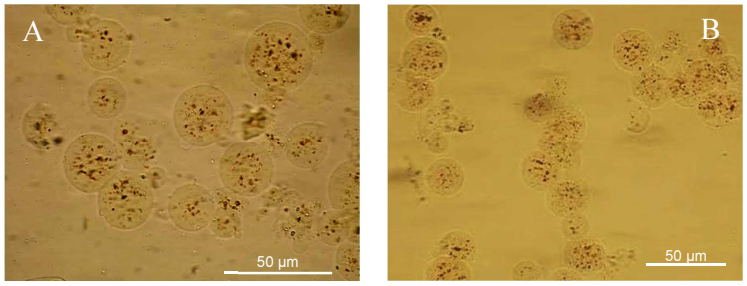

Figure S3: Optical microscopic images of Fe_3O_4@Ch-AuNPs (A) and Fe_3O_4@Ch-PdNPs (B).

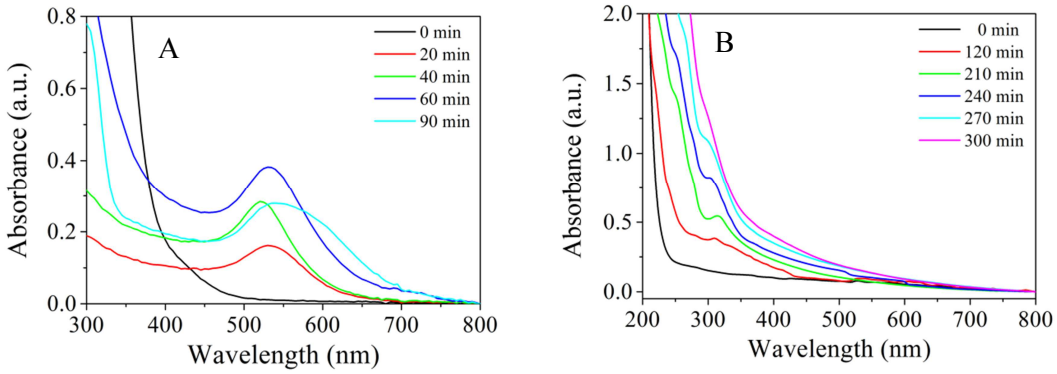

Figure S4: Optimization of synthesis of Fe_3O_4@Ch-AuNPs (A) and Fe_3O_4@Ch-PdNPs (B).

PN-I-219 RESULTS (1st CYCLE)

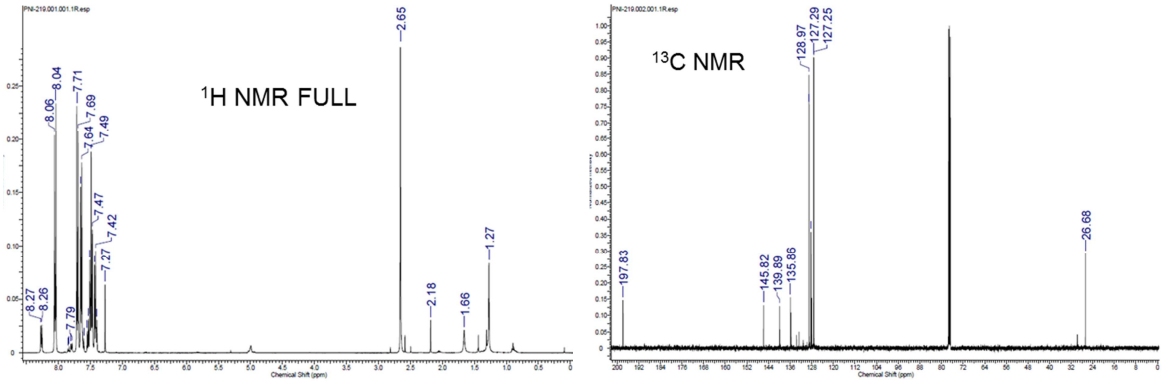

Figure S5: Representative NMR spectra of the product from reaction mixture (heating at 50 °C for 1 h, 1st cycle)

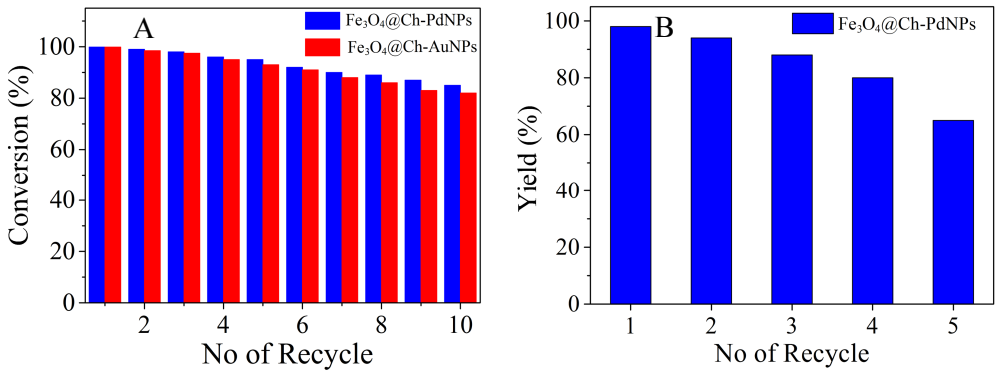

Figure S6: Recyclability of Fe_3O_4@Ch-MNPs in hydrogenation (A) and Suzuki coupling (B) reaction.

Table S1: Comparison of Apparent Rate Constants of Fe_3O_4@Ch-MNPs (M=Au and Pd) with Chemically Synthesized MNPs for Methylene Blue Reduction

Nanocomposite	Size	Condition	K_{app}(/ min)	References
Fe_3O_4@Ch-PdNPs	20 ± 2.9 µm	Visible light	1.04*	Present study
Fe_3O_4@Ch-PdNPs	20 ± 2.9 µm	UV light	5.04*	Present study
Fe_3O_4@Ch-AuNPs	22 ± 3.1 µm	Visible light	5.4×10^{-1}*	Present study
Fe_3O_4@Ch-AuNPs	22 ± 3.1 µm	UV light	4.05*	Present study
Ag/MFC	340 nm	25 °C	3.4×10^{-1}	[1]
Au:TiO_2	90 nm	UV light	11.4×10^{-3}	[2]
Ag:TiO_2	50 nm	UV light	7.1×10^{-3}	[2]
Cu:TiO_2	35 nm	UV light	17.3×10^{-3}	[2]
Au:TiO_2	90 nm	Visible light	6.5×10^{-3}	[2]
Ag:TiO_2	50 nm	Visible light	4×10^{-3}	[2]
Cu:TiO_2	35 nm	Visible light	5.5×10^{-3}	[2]
Pd/TiO_2 NTs	220 nm	Stimulated solar light	1.85×10^{-2}	[3]
ZnO Nanorods	5–7 nm	Visible light	1.948×10^{-2}	[4]

*Conditions: Methylene blue (10 mL, 20 mg/L), $NaBH_4$ (2.9 mM), Fe_3O_4@Ch-MNPs (2 ± 0.5 mg, containing 2.6% Pd in Fe_3O_4@Ch-PdNPs and 5.8% Au in Fe_3O_4@Ch-AuNPs), pH 7.2

Table S2: Comparison of rate constants of Fe_3O_4@Ch-MNPs (M=Au and Pd) in *p*-Nitrophenol hydrogenation reaction with chemically synthesized MNPs

Nanocomposite	Size	k_{nor}	Ref.
Fe_3O_4@Ch-PdNPs	20 ± 2.9 µm	4.9 ± 0.3 /mmol/s*	Present study
Fe_3O_4@Ch-AuNPs	22 ± 3.1 µm	3.3 ± 0.5 /mmol/s*	Present study
Ammonium bismuth citrate synthesized AuNPs	20 – 140 nm	2.1×10^{-3} /mmol/s	[5]
Tri-sodium citrate synthesized AuNPs	20 – 50 nm	1×10^{-3} /mmol/s	[5]
Silver nanodentrites	60 – 120 nm	3.04×10^{-1} /mmol/s	[6]
PCo_2Ni_1	52 ± 9 nm	6.68×10^{-2} /mmol/s	[7]
PNi	44 ± 12 nm	4.57×10^{-2}/mmol/s	[7]
Au-Pt BimetalicNanorod	Width: 7.4 ± 0.8 nm; Length: 39.5 ± 6.5 nm	1.40×10^{-1} L/s/m^2	[8]
Au Nanorod	Width: 6.6 ± 0.3 nm; Length: 34.5 ± 5.2 nm	2.10×10^{-1} L/s/m^2	[8]
Palladium Clusters	4 – 5 nm	1.33×10^{-4} L/s/m^2	[9]

*Conditions: *p*-Nitrophenol (0.1 mL, 3×10^{-3} M), $NaBH_4$ (0.1 mL, 0.3 M), Fe_3O_4@Ch-MNPs (5 ± 0.1 mg, containing 2.6% Pd in Fe_3O_4@Ch-PdNPs and 5.8% Au in Fe_3O_4@Ch-AuNPs), reaction temperature at 30 °C

Table S3: Comparative study of TON and TOF for Suzuki coupling reaction those are reported values with our results.

R_1	X	R_2	Reaction condition:	Yield (%)	TON	TOF	Ref
$COCH_3$	I	H	Refluxing/ H_2O/ Fe_3O_4@Ch-PdNPs/ 540 min/ 100°C	99	50769	5641*	Present study
$COCH_3$	I	H	Sunlight/ H_2O/ Fe_3O_4@Ch-PdNPs/ 300 min/ 37± 3°C	73	37435	7437*	Present study
$COCH_3$	I	H	Lab condition/H_2O/ Fe_3O_4@Ch-PdNPs/ 45min/ 52 ± 1°C	90	46153	61538*	Present study
$COCH_3$	I	H	Microwave/ H_2O/ Fe_3O_4@Ch-PdNPs/ 60 min/ 50 ± 2°C	98	50256	50256*	Present study
H	I	m-CH_3	Stirring/EtOH–H_2O (1:1)/ CB[6]-PdNPs/ 300 min/room temperature	89	1780	3560	[10]
H	Br	o-Py	Stirring/EtOH–H_2O (1:1)/ CB[6]-PdNPs/ 300 min/room temperature	8	1600	320	[10]
H	I	H	H_2O/EtOH (1:1)/Poly-(sodium sulfonate-triazolymethyl)–styrene stabilized PdNPs/ 24 h / 25 °C	82	990	1980	[11]
H	I	H	MeOH (2:1)/Dendrimer-encapsulated PdNPs (1 mol % Pd)/$CHCl_3$/ 24 h/ 25 °C	68	68	17	[12]
H_3CO	I	$B(OH)_2$	Refluxing/ H_2O/ Fe_3O_4@PUNP/ 60 min/ 90 °C	95	950	950	[13]
$COCH_3$	I	2-Me	H_2O/0.1% Pd-FSG/300 min/100 °C	90	3780	158	[14]
H	I	CO_2Me	Aerobic/ DMF/ PdNPs/ 90 min/ 110 °C	>99	10000	6667	[15]
4-MeO	Br	CO_2Me	Aerobic/ DMF/ PdNPs/ 540 min/ 130 °C	57	114	13	[15]
$COCH_3$	Br	$B(OH)_2$	Microwave irradiation/H_2O/HNT-PNIPAAM/ PdNPs/10 min/ 120 °C	>95	6250	37500	[16]
$COCH_3$	I	$B(OH)_2$	Microwave irradiation H_2O/HNT-PNIPAAM/ PdNPs/10 min/120 °C	94	5880	35250	[16]
H	I	Ph	Solvent free/ H_2O / PS-ppdot-Pd(II)(1)/ 180 min/ room temperature	97	96	32	[17]
4-OMe	I	H	XG-Pd, K_2CO_3 /12 h/ 90 °C	60	391	32	[18]
H	I	$CH_3CH_2CH_2^-$	H_2O/ Pd–Fe–H (2)/360 min/ 80 °C	96	45	5	[19]
H	I	Ph	Solvent free/diatomit-supported Pd(II) salophen complex(0.3)/ 300 min/ room temperature	97	320	64	[20]

*Conditions: Phenylboronic acid (183 mg, 1.5 mmol), *p*-Iodoacetophenone (246.5 mg, 1 mmol), K_2CO_3 (276.5 mg, 2 mmol), Fe_3O_4@Ch-PdNPs (8 ± 0.5 mg, containing 2.6% Pd), H_2O and under aerobic condition.

References

1. Zhu, M.; Wang, C.; Meng, D.; Diao, G. In Situ Synthesis of Silver Nanostructures on Magnetic Fe_3O_4@C Core–Shell Nanocomposites and their Application in Catalytic Reduction Reactions. *J. Mater. Chem. A* **2013**, *1*, 2118–2125.
2. Sangpour, P.; Hashemi, F.; Moshfegh, A. Z. Photoenhanced Degradation of Methylene Blue on Cosputtered M:TiO_2 (M = Au, Ag, Cu) Nanocomposite Systems: A Comparative Study. *J. Phys. Chem. C* **2010**, *114*, 13955–13961.
3. Zhang, Z.; Yu, Y.; Wang, P. Hierarchical Top–Porous/Bottom–Tubular TiO_2 Nanostructures Decorated with Pd Nanoparticles for Efficient Photoelectrocatalytic Decomposition of Synergistic Pollutants. *ACS Appl. Mater. Interfaces* **2012**, *4*, 990−996.
4. Baruah, S.; Mahmood, M. A.; Myint, M. T. Z.; Bora, T.; Dutta, J. Enhanced Visible Light Photocatalysis through Fast Crystallization of Zinc Oxide Nanorods. *Beilstein J. Nanotechnol*. **2010**, *1*, 14–20.
5. Das, S. K.; Dickinson, C.; Lafir, F.; Brougham, D. F.; Marsili, E. Synthesis, Characterization and Catalytic Activity of Gold Nanoparticles Biosynthesized with *Rhizopus oryzae* Protein Extract. *Green Chem*. **2012**, *14*, 1322–1334.
6. Zhang, W.; Tan, F.; Wang, W.; Qiu, X.; Qiao, X.; Jianguo Chen, J. Facile, Template–Free Synthesis of Silver Nanodendrites with High Catalytic Activity for the Reduction of *p*-Nitrophenol. *J. Hazard. Mater*. **2012**, *217*, 36–42.
7. Rashid, M. H.; Raula, M.; Mandal, T. K. Polymer Assisted Synthesis of Chain–like Cobalt–Nickel Alloy Nanostructure: Magnetically Recoverable and Reusable Catalysts with High Activities. *J. Mater. Chem*. **2011**, *21*, 4904–4917.
8. Lu, Y.; Yuan, J.; Polzer, F.; Drechsler, M.; Preussner, J. In Situ Growth of Catalytic Active Au−Pt Bimetallic Nanorods in Thermoresponsive Core−Shell Microgels. *ACS Nano* **2010**, *4*, 7078–7086.
9. Halder, A.; Patra, S.; Viswanath, B.; Munichandraiah, N.; Ravishankar, N. Porous, Catalytically Active Palladium Nanostructures by Tuning Nanoparticle Interactions in an Organic Medium. *Nanoscale* **2011**, *3*, 725–730.
10. Karami, K.; Naeini, N. H. Palladium Nanoparticles Supported on Cucurbit [6] uril: an Efficient Heterogeneous Catalyst for the Suzuki Reaction under Mild Conditions. *Appl. Organometal. Chem*. **2015**, *29*, 33–39.
11. Ornelas, C.; Diallo, A. K.; Ruiz, J.; Astruc, D. "Click" Polymer-Supported Palladium Nanoparticles as Highly Efficient Catalysts for Olefin Hydrogenation and Suzuki Coupling Reactions under Ambient Conditions. *Adv. Synth. Catal*. **2009**, *351*, 2147–2154.
12. Diallo, A.; Ornelas, C.; Salmon, L.; Aranzaes, J. R; Astruc, D. "Homeopathic" Catalytic Activity and Atom−Leaching Mechanism in Miyaura–Suzuki Reactions under Ambient Conditions with Precise Dendrimer–Stabilized Pd Nanoparticles. *Angew. Chem. Int. Ed.* **2007**, *46*, 8644–8648.
13. Yang, J.; Wang, D.; Liu, W.; Zhang, X.; Bian, F.; Yu, W. Palladium Supported on a Magnetic Microgel: an Efficient and Recyclable Catalyst for Suzuki and Heck Reactions in Water. *Green Chem*. **2013**, *15*, 3429−3437.
14. Bernini, R.; Cacchi, S.; Fabrizi, G.; Forte, G.; Petrucci, F.; Prastaro, A.; Niembro, S.; Shafir, A.; Vallribera, A. Perfluoro–Tagged, Phosphine–Free Palladium Nanoparticles

Supported on Silica Gel: Application to Alkynylation of Aryl Halides, Suzuki–Miyaura Cross–Coupling, and Heck Reactions under Aerobic Conditions. *Green Chem*. **2010**, *12*, 150−158.

15. Diego, W.; Alonso, A.; Najera, C. Oxime-Derived Palladacycles as Source of Palladium Nanoparticles. *Chem. Soc. Rev*. **2010**, *39*, 2891–2902.
16. Massaro, M.; Schembri, V.; Campisciano, V.; Cavallaro, G.; Lazzara, G.; Milioto, S.; Noto, R.; Parisib, F.; Riela, S. Design of PNIPAAM Covalently Grafted on Halloysite Nanotubes as a Support for Metal-Based Catalyst. *RSC Adv*. **2016**, *6*, 55312−55318.
17. Bakherad, M.; Keivanloo, A.; Bahramian, B.; Jajarmi, S. Copper- and Solvent-Free Sonogashira Coupling Reactions of Aryl Halides With Terminal Alkynes Catalyzed by 1-phenyl-1,2-propanedione-2-oxime Thiosemi-Carbazone-Functionalized Polystyrene Resin Supported Pd(II) Complex under Aerobic Conditions. *Appl. Catal. A* **2010**, *390,* 135−140.
18. Maity, M.; Maitra, U. An Easily Prepared Palladium–Hydrogel Nanocomposite Catalyst for C–C Coupling Reactions. *J. Mater. Chem. A* **2014**, *2*, 18952–18958.
19. Li, H.; Zhu, Z. H.; Li, H. X.; Li, P.; Zhou, X. G. Recyclable Hollow Pd–Fe Nanospheric Catalyst for Sonogashira-, Heck-, and Ullmann-Type Coupling Reactions of Aryl Halide in Aqueous Media. *J. Colloid. Interf. Sci.* **2010**, *349,* 613−619.
20. Bahramian, B.; Bakherad, M.; Keivanlo, A.; Bakherad, Z.; Karrabi, B. The First Heterogeneous Sonogashira Coupling Reaction of Aryl Halides With Terminal Alkynes Catalyzed by Diatomite-Supported Palladium(II) Salophen Complex. *Appl. Organomet. Chem*. **2011**, *25*, 420−423.